Simulation Study for Developing Anidolic Solar Shading for Warm-Humid Climates

Floriberta Binarti[1], Jackobus A. Prasetya[1]
[1]Architecture Department, Universitas Atma Jaya Yogyakarta, Yogyakarta, Indonesia

Abstract

Installation of solar shading device in warm-humid climates for preventing overheating tends to generate gloomy interior. Hence, adopting the anidolic principles on an exterior solar shading, namely anidolic solar shading (ASS), aimed to create bright, pleasant interior and to improve the thermal performance of the anidolic daylighting system (ADS). This study developed a simulation-based parametric method to examine the critical elements of the anidolic collector and to investigate the magnitude of the improvement impacts on the energy performances of the ASS relative to the performances of unshaded clerestory, clerestory with eave, and ADS. By adding cavities and self-shading, the ASS could achieve relatively high thermal and daylighting performance estimated by simulation study, which comparatively agree quite well with the short-term monitoring results.

Introduction

External solar shading has been widely applied as an effective strategy to reduce solar heat gain that majorly contributes to the space cooling load in warm-humid climates. How to create bright, pleasant space of the building installed with the external shading, however, remains difficult, but challenging to achieve. Even the current state of the art of shading system, Electrochromic (EC) window, still creates gloomy indoor space in the whole year because the EC window reduces the transparency to adjust to outdoor conditions during clear sky conditions. To answer this challenge, this study proposed a new external shading with high daylighting performance and very low thermal impact. The idea of developing this device aimed to improve the thermal performance of the anidolic daylighting system (ADS) for warm-humid climates. Renowned as a highly efficient daylighting system (Scartezzini and Courret, 2002), the ADS comprises three components, i.e. anidolic collector, light tunnel, and distributor/diffuser. Working based on the edge-ray principles, the ADS could create bright nuance (Binarti and Satwiko, 2016), but still transmitted excessive solar heat radiation (Binarti, 2015).

Methods

Simulation-based parametric study

The thermal performance improvement of ADS, namely anidolic solar shading (ASS), was expected to protect the lower part of the clerestory glazing against direct solar radiation from the low altitude sun, meanwhile to deflect the zenithal light into the indoor space. Previous studies on ADS (Wittkopf et al., 2010; Binarti and Satwiko, 2015) defined three parameters of anidolic collector, which determine their daylighting and thermal performance, i.e. opening height, collector width and angular spread. For developing a high performance ASS, a parametric study (see Figure 1) was designed by employing computational simulations to predict the daylighting and thermal performance of a building equipped with the ASS varying in three parameters, relative to the same building equipped with unshaded clerestory (UC), clerestory with eave (CE) and ADS. Because each step of the development posses specific energy transfer modes, selecting proper simulation engines was required for the reliable results.

Daylight Factor (DF) can function as a single value to estimate the daylighting performance in a whole year regardless the climate, time and orientation. Dissatisfactions with the results, however, revealed vastly due to underestimated predictions (Ng, 2001; Mardaljevic, 2004; Kleindienst, 2006). To solve this problem, Reinhart and Walkenhorst (2001) developed a climate-based sky luminance, so called Daysim, that interpolates direct solar contributions for particular sky conditions from four neighbouring, representative sky conditions (Reinhart and Brexton, 2009). Daylight autonomy (DA), the first annual daylighting metric calculated by Radiance/Daysim, was used in this study to complement the DF simulations.

Previous study on various ADS sizes showed that the space solar heat gain (SHG) dominated the ADS thermal performance (Binarti, 2015). However, installing the anidolic collector as external shading device might modify the portion of radiative and convective heat transfer through the glass pane. To examine the heat transfer mode, which contributes to the ASS thermal performance, the space SHG and cooling load (CL) for air conditioned buildings, aside from the indoor air temperature (Ti) for naturally ventilated buildings, must be partially analyzed using EnergyPlus (Crawley et al., 2013). Due to the limitation of EnergyPlus in simulations of the thermal behaviour of ASS in detail, refinements of the thermal simulations employed computational fluid dynamic (CFD).

In this study, all fenestration models (UC, CE, ADS and ASS) were installed in the same position on an 8m-wide (R), 6m-long, and 3.2m-high (H) room to represent classrooms or open offices. The building models equipped with ASS and ADS vary with the aperture height (O: 70 cm, 75 cm, and 80 cm), collector width (W: 91 cm, 108 cm, 118 m, and 128 cm), and collector's angular spread (A: 45^o, 52^o, and 60^o). All models were built from the same materials and the same surface reflectances with the internal reflectances complying with the maximum value of IESNA recommendations (Rea,

2000). Whereas, the anidolic collectors were made of stainless steel sheets (k: 17 W/m.K; c: 460 J/kg.K; ε: 0.3) proven by Praditwattanakit et al. (2013) and Binarti and Satwiko (2016) as a high reflectance and affordable material. The eave used the same roof material, i.e. asbestos cement sheets (k: 0.36 W/m.K; c: 1050 J/kg.K).

Yogyakarta (110°26'E and 7°32'S) and Singapore (1.4°N and 104°E) were selected to represent a warm-humid city in the southern hemisphere and the northern hemisphere respectively. Two aperture orientations were chosen based on the previous studies on ADS performance in Yogyakarta (Binarti, 2016) and in Singapore (Linhart et al., 2010).

The weather profiles of both cities provided by EnergyPlus displayed similarities in the dry-bulb and dew-point temperature profile. In Yogyakarta the solar radiation was dominated by direct normal irradiance. Despite the higher total solar radiation, Yogyakarta had lower diffuse horizontal solar radiation than Singapore that was dominated by the diffuse horizontal solar radiation. In Singapore, high wind velocity occurred all year round, while in Yogyakarta high wind velocity only appeared in August and September.

Although sky type in warm climates is often described as predominantly overcast sky (Hyde, 2008), some measurements showed differently. Based on measurements of the cloud cover ratio by Rahim and Mulyadi (2004), sky in Makassar (119° E, 5.8° N), Indonesia was dominated by intermediate sky (69.80%). However, 6-month monitoring of ADS application in Yogyakarta (Binarti and Satwiko, 2016) recorded that clear sky with the sun most frequently appeared during the monitoring. Meanwhile, Linhart et al. (2010) mentioned that the standard overcast sky (33%) and overcast sky (28%) dominated the sky in Singapore.

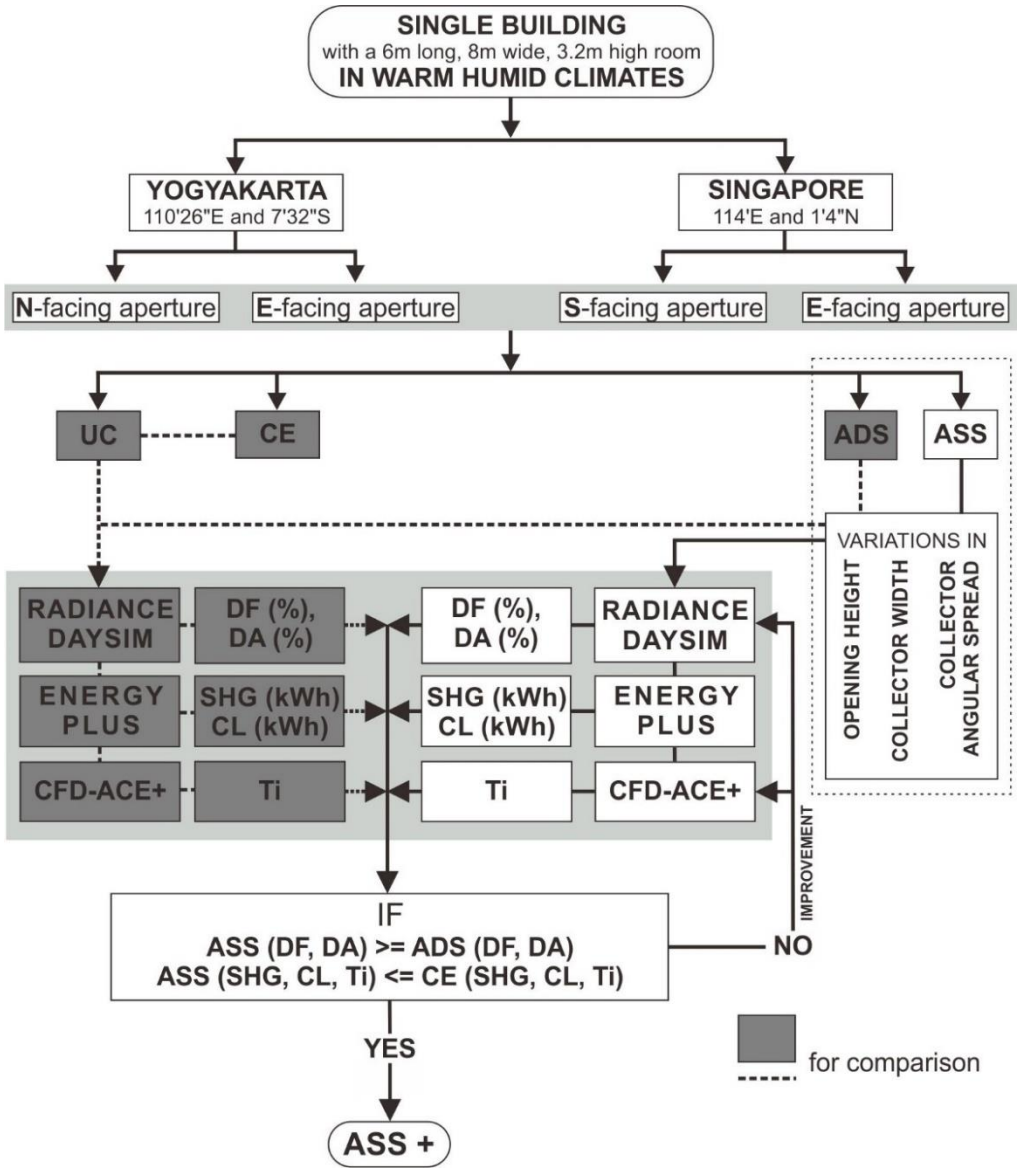

Figure 1: Simulation-based parametric approach.

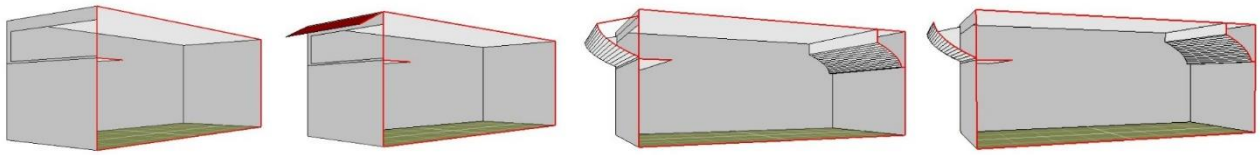

Figure 2: Fenestration models from left to right: UC, CE, ADS and ASS.

EnergyPlus for thermal simulations

EnergyPlus, a current widely used building energy simulation engine, relies on zone heat balance method for thermal load calculations. For calculation of the space thermal/CL in a single building with glazing window in warm-humid climates, SHG becomes the most important component. EnergyPlus uses Perez solar radiation model to split global solar radiation into direct normal and diffuse horizontal components. An anisotropic radiance distribution model of the sky is provided to calculate the transmittance of sky radiance. Empirical validation conducted by Loutzenhiser et al. (2008) proved that the SHG algorithm in EnergyPlus performed well in modelling solar gain transmitted through a solar selective glazing unit with exterior Venetian blinds and interior mini-blinds at two different slat positions.

Shades from the building/external elements on the aperture may significantly contribute to the SHG. In EnergyPlus, shading calculations rely on methods based on projection and clipping operations (P&C methods) (Maestre, 2012). This study selected "full exterior and interior with reflection" shading model to compute the amount of beam radiation falling on each surface in the zone by projecting the sun's rays through the exterior windows and with regards to the effect of exterior shadowing surfaces and shading devices.

Convective heat transfer may change the window surface temperature. Hence, selection of the convective heat transfer model should consider the exterior/interior conditions. This study selected adaptive convection algorithm to calculate the exterior (ECHTC) and interior (ICHTC) convective heat transfer coefficient because this model can dynamically manage the selection of ECHTCs and ICHTCs, which are most appropriate for a given surface at a given time (UIUC and LBNL, 2015).

Table 1: EnergyPlus simulation set-up

site	Exposure to wind	normal
air conditioned space	AC system	Split no fresh air
	Cooling system COP	1.83
	Cooling set point	26 ^{o}C
	Airtightness: model infiltration	Scheduled, constant rate: 1 ac/h
naturally ventilated space	System	No heating/cooling
	Wind factor	1
	Airtightness: model infiltration	Calculated, good, constant rate: 1 ac/h

All 3D-models were built using DesignBuilder that comprised one thermal zone and component block(s) for the external shading device. The eave of CE model was built from a component block. Because the ASS functions as external shading device, the ASS collector was constructed from several segmented planes forming one curved component block and two planar component blocks. However, the modeling ADS collector was treated differently. The ADS collector was created using a zone, that further was merged with the building zone.

Radiance/Daysim for daylighting simulations

Relying on a backward ray-tracing, Radiance (Ward, 2002) can achieve reasonably accurate results of lighting simulations. These methods support Radiance in handling specular direct and indirect component calculations that occur in the anidolic collector in high accuracy. The critical restriction of Radiance in modeling the parabolic collector lies in the reflection of intense light from curved specular surfaces. Computing such system, however, requires a forward ray tracing method (Chadwell, 1997). To improve the accuracy, constructing high resolution segmented curve of a parabolic model was suggested by Compagnon (Kleindienst, 2006). In this study the 3D-models of the anidolic collector were created from 5cm-wide surfaces arranged in parallel using Ecotect (Marsch, 2005).

Table 2: Daysim simulation set-up

Ambient bounces	5	Specular jitter	1.0000
Ambient division	1000	Limit weight	0.004000
Ambient super-samples	20	Direct jitter	0.0000
Ambient resolution	300	Direct sampling	0.200
Ambient accuracy	0.1	Direct relays	2
Limit reflection	6	Direct pre-test density	512
Specular threshold	0.1500		

CFD-ACE+ for thermal simulation refinement

CFD-ACE+ (ESI Group, 2014) was employed to obtain a detailed thermal analysis of the complicated ASS models. The simulations used the k-ε standard turbulence model with Reynolds Averaged Navier-Stokes (RANS) mathematical approach to solve turbulent problems with mean value and averaged operation. The conductive heat transfer was computed using a combination of pure conduction model to solve the pure conduction problems

and conjugate heat transfer model to accommodate the heat transfer from solid to fluid or otherwise. All simulations were set up under 28.5 ºC for the ambient temperature, 45º for the solar altitude, 600 W/m^2 for the solar radiation. This solar altitude represents the sun position at around 9 a.m. in equator (September 21 for north-facing windows). The wind velocity varied from 0.1, 0.5 up to 1.0 m/s.

Three radiation models were implemented to calculate radiative heat transfer through the glass pane during CFD simulation study. At first, Surface To Surface model (STS) was implemented because this radiation model has been well known of its capability of including sun radiation into the model as well as providing good accuracy in predicting surrounding thermal behaviour inside the calculation domain by the simplest rules. Because STS does not account for radiation, which propagates in multiple directions and does not support transluscent properties, Discrete Ordinate Model (DOM) was implemented on the second stage of CFD simulations by dividing the radiation spectrum into 0 nm, 0.3 nm, 0.7 nm, and 3 nm.

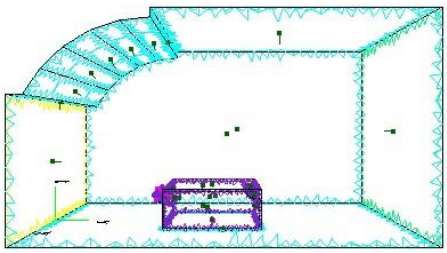

Figure 3: The solar radiation model in CFD-ACE+ for ASS simulations.

On the third stage, Monte Carlo model (MC) was selected to treat all directions of radiative transfer in a continuous fashion and simulate strong oscillations in spectral (specular) radiative properties. The iteration of the MC used 1,000,000 rays.

Results and discussion

Daylighting performance simulation results

From the annual percentages of the daylighting level (the DA and DF) of the four fenestration models presented in Figure 4, DF simulation results demonstrated a similar pattern with the DA's. By comparing the simulation results of both cities, significant differences between the DA of the models in Yogyakarta and those in Singapore are noticed. Despite the closer location to the equator, all models in Singapore created a lower DA than those in Yogyakarta. The overcast sky that dominated the sky luminance in Singapore might cause these results.

Changing the collector orientation insignificantly modified the DA of both locations, although it can be concluded that east-facing collectors performed better than north/south-facing collectors. Generally, ASS insignificantly improved (1-3%) the DA compared to the DA of ADS, especially to the north-facing collector in Yogyakarta. However, the ASS performed the best, especially compared to the performance of CE (100%) for most collector and aperture geometries/sizes.

In general, the ASS achieved the highest daylighting performance even compared to the performance of the ADS. For the narrow collectors (W091), the highest DA was attained by the ASS with 45º angular spread collector and 80cm-height aperture. Wider collectors received more skylight, which produced higher DA, but also potentially accumulate higher solar heat gain. Increasing the aperture height raised (avg) 4% of the DA and (avg) 5% of the DF. Meanwhile, the increasing the collector's angular spread could raise the DA. More significant increasing of the DA (avg. 1.37%) occured when the angular spread changed from 45º to 52º.

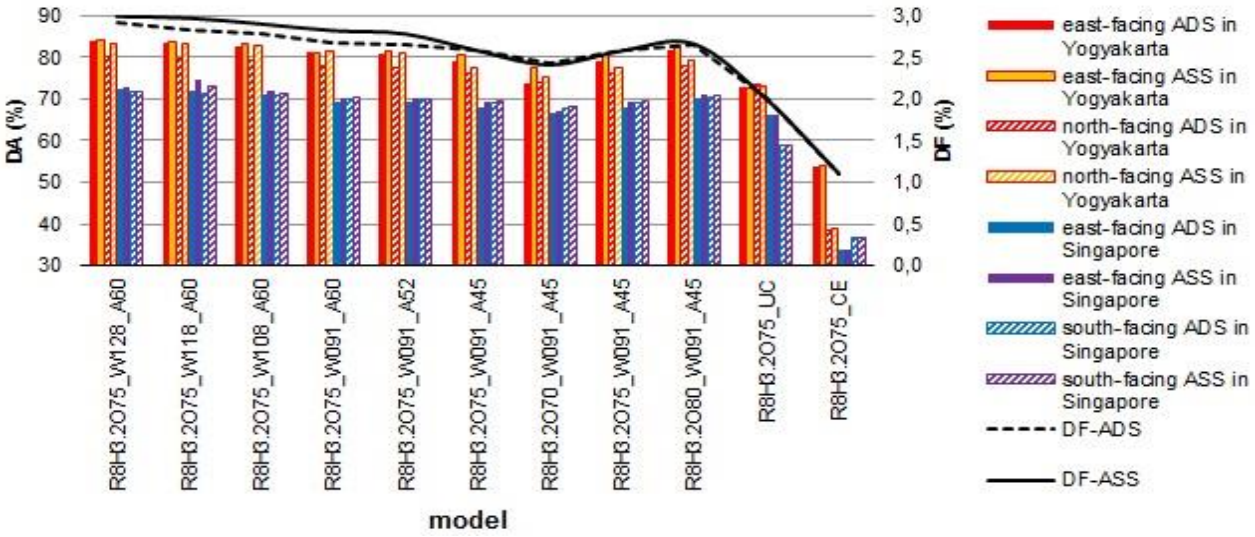

Figure 4: DF and DA of Unshaded Clerestory (UC), Clerestory with Eave (CE), Anidolic Daylighting System (ADS), Anidolic Solar Shading (ASS) in Yogyakarta and Singapore.
(Notes: R: room width, H: room height, O:opening height, W: collector width, A: collector's angular spread)

Simulations of ASS thermal performance

Replacement of the ADS with ASS decreased 54-58 kWh/m^2 of the SHG (see Figure 5 and 6). Highest reduction (58 kWh/m^2) was created by the north-facing ASS in Yogyakarta. However, this replacement only slightly reduced the CL (13-14 kWh/m^2 in Yogyakarta and 23 kWh/m^2 in Singapore) and Ti (0.13-0.38 degC).

Figure 6 explains that EnergyPlus simulation results of ASS in Singapore demonstrated consistent results. Narrow collectors (91 cm) with 52^o angular spread in Singapore achieved the lowest SHG, CL and Ti than other collectors. In contrast, the simulations of ASS in Yogyakarta exhibited slightly inconsistent effect of the collector width and angular spread on the SHG, CL and Ti. Figure 5 describes that reduction of the SHG was not followed by the reduction of CL and Ti.

In general, narrow collector of the east-facing ASS could reduce the SHG below the SHG of the east-facing UC, but still above the SHG of the east-facing CE. It can be concluded, however, that ASS collector's width, angular spread and aperture's height insignificantly modified the CL, Ti, and SHG.

Only insignificant impact on the SHG, CL and Ti was noticed when the aperture height changed. Therefore, increasing the aperture height (80 cm) was considered to be strategic in terms of the thermal and daylighting performance (see **Daylighting performance simulation results**).

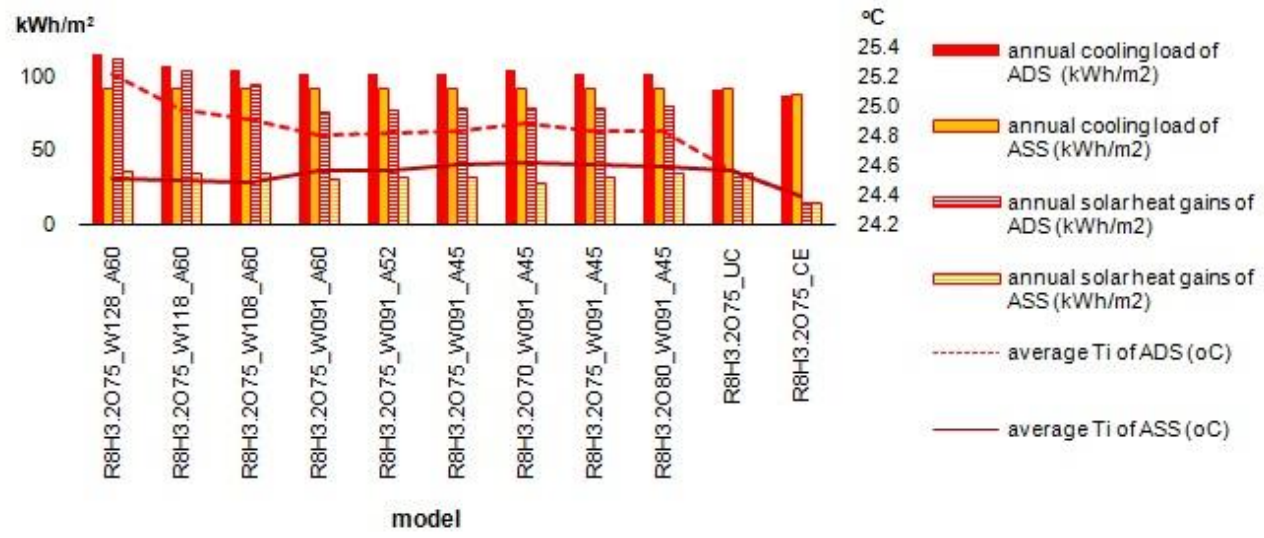

Figure 5: EnergyPlus simulations of east-facing UC, CE, ADS and ASS in Yogyakarta.

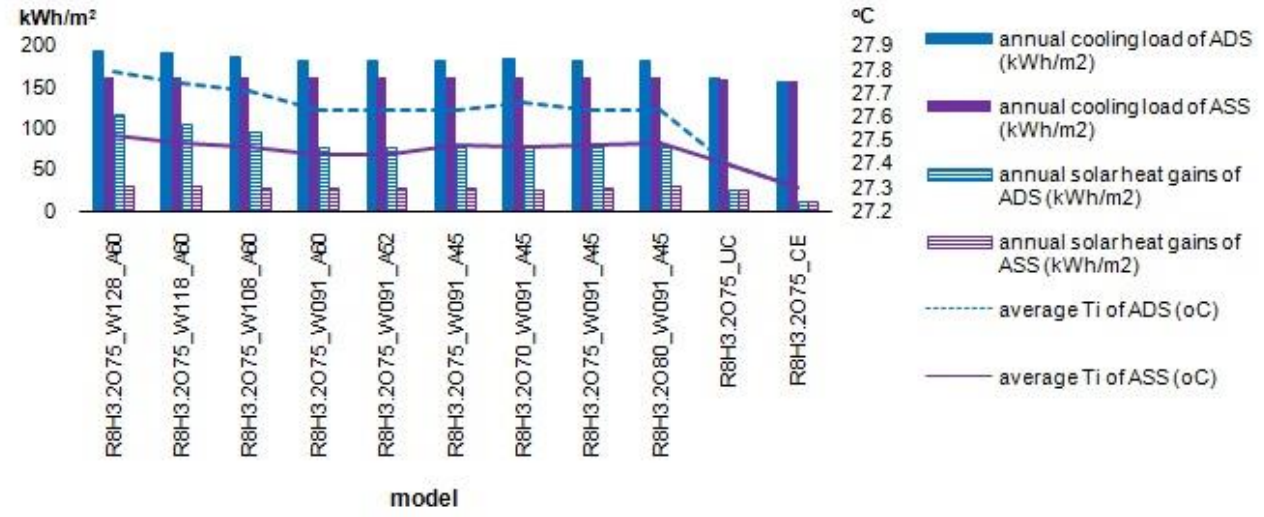

Figure 6: EnergyPlus simulations of south-facing UC, CE, ADS and ASS in Singapore.

To obtain more convincing thermal analysis, the next step employed CFD-ACE+. Figure 7 depicts the temperature contours in the building equipped with UC, CE, ADS, and ASS that present respectively the average Ti as follows: 36.93 ºC, 35.99 ºC, 38.45 ºC, and 37.30 ºC. Compared to the CFD simulation results, EnergyPlus seemed to overestimate the Ti of the room equipped with ADS. Nevertheless, average Ti of the building equipped with UC, CE, ADS and ASS simulated by EnergyPlus has the same order as the Ti simulated by CFD-ACE+.

The improvements of ASS thermal performance

Unfortunately, the modification of the ADS as external shading on the first step could not achieve the goal as shown in Figure 8. Although the SHG of the ASS was significantly decreased, the CL and Ti of the ASS were estimated higher than those of UC and CE. Convective heat transfer might cause high CL and Ti of the ASS. Improvements of the ASS collector, hence, were required to reduce the convective heat transfer through the glass pane.

The first solution was adding continuous cavity between the collector and the wall, so called "bottom vented ASS" or ASS_v1. The bottom vent also functions to drain the rain water falling on the collector body. This solution, however, only decreased 0.22 degC of the average Ti (see Figure 8). To dissipate the heat inside the collector (on the external surface of the clerestory glazing), adding cavities on the collector body was proposed as the second solution. This modification, namely "porous ASS" or ASS_v2, also produced a slight reduction of the average Ti (0.15 degC). Figure 8 shows that the buildings equipped with ASS_v1 and ASS_v2 were estimated to create 37.08 ºC and 36.93 ºC of the average Ti respectively.

The ineffective solutions above, i.e. ASS_v1 and ASS_v2, led to a decision to propose shelf shading for decreasing the solar heat gain through the ASS clerestory. Moving the clerestory to a deeper side could provide more shade on the glass pane. This improvement, namely "ASS_v3" or "ASS+", resulted in significant reduction of the average Ti as presented in Table 3 and Figure 9. ASS+ with any angular spread significantly reduce the Ti below the Ti of the CE. ASS+ with 52º angular spread performed the best with insignificant temperature difference.

Table 3: Average indoor air temperature of a building equipped with porous ASS with various angular spread under various wind velocity

model	Wind velocity		
	0.1 m/s	0.5 m/s	1 m/s
R8H3.2080_W091_A45_v3	28.94	28.94	28.94
R8H3.2080_W091_A52_v3	28.94	28.94	28.92
R8H3.2080_W091_A60_v3	28.97	28.97	28.96

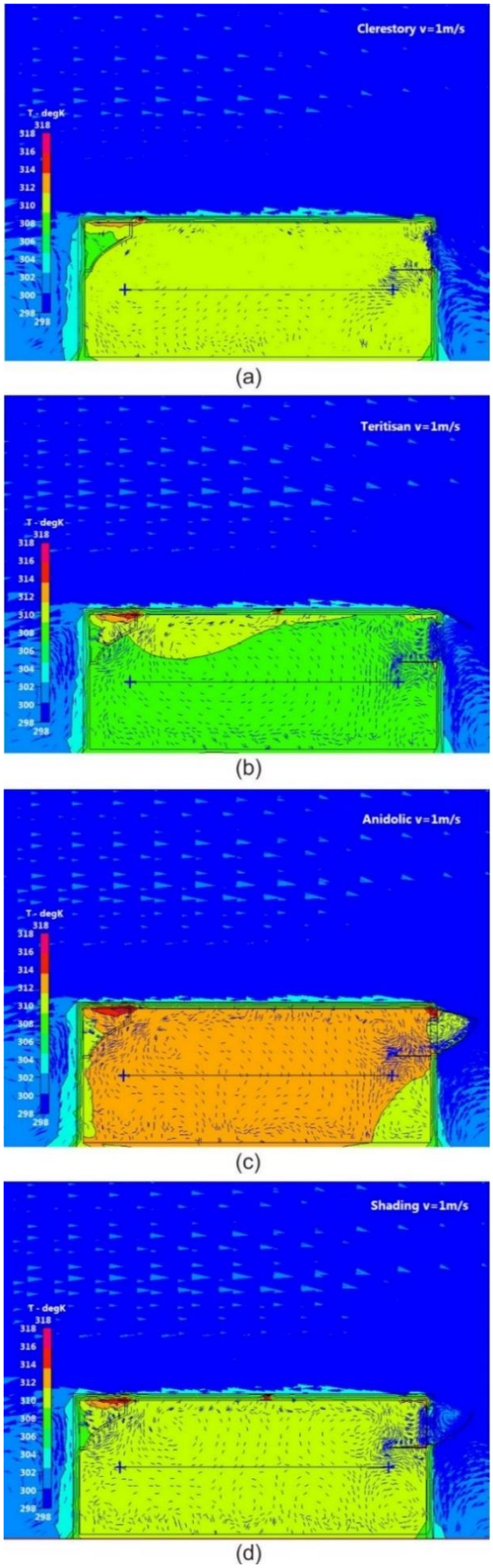

Figure 7: Temperature contours inside a building equipped with UC (a), CE (b), ADS (c), and ASS (d) under 1 m/s of wind simulated by CFD.

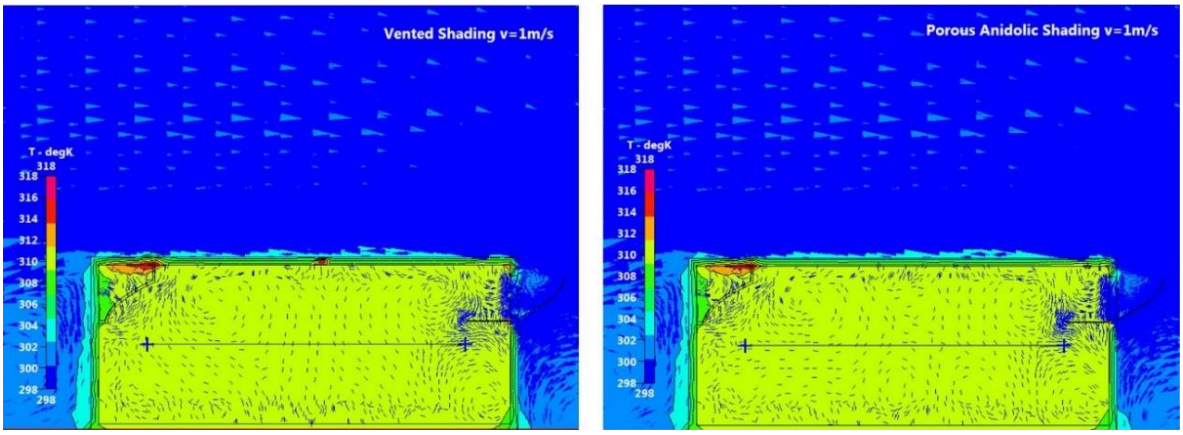

Figure 8: Indoor air temperature contours of a building equipped with ASS_v1 (left) and with ASS_v2 (right) simulated by CFD under 1 m/s of wind.

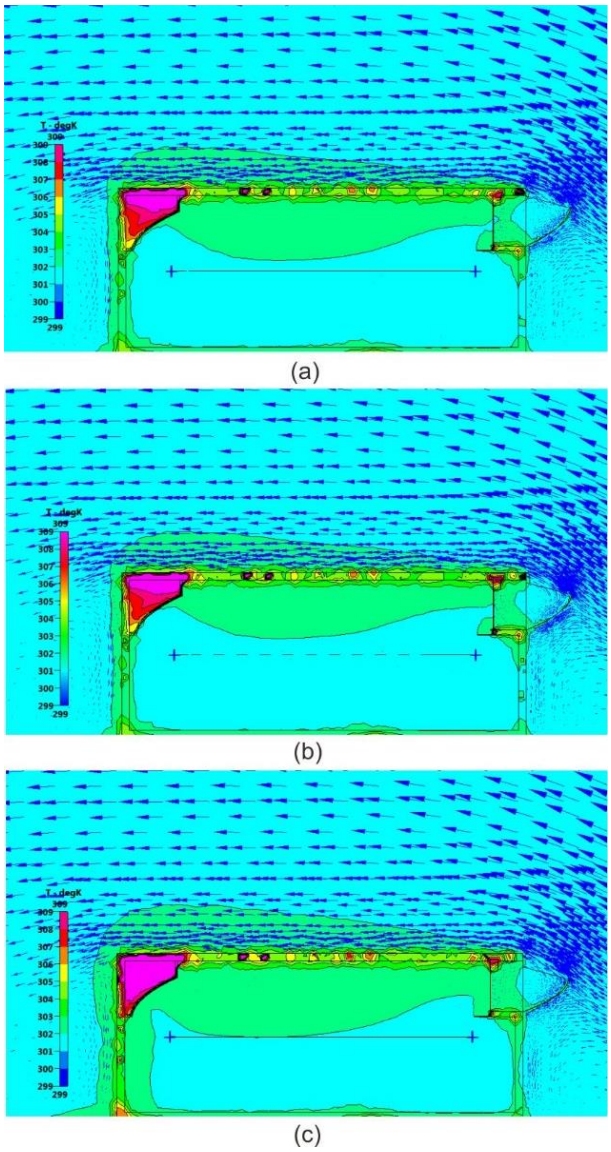

Figure 9: Indoor air temperature contours of a building equipped with 45°-ASS+ (a), 52°-ASS+ (b), and 60°-ASS+ (c) *simulated by CFD under 1 m/s of wind.*

The ASS+ daylighting performance

Similar patterns of the DA and DF can be observed from simulation results of a building equipped with ADS or ASS in Figure 10. Adding cavities of the collector body arose the DA up to 2.5%, except for the south-facing ASS_v2 in Singapore. These cavities allowed more low-altitude direct sunlight to enter the indoor space. Meanwhile, moving the clerestory to a deeper side only changed the position of the glass pane, but kept the travel length of the light beam through the glass pane. This modification could even provide a larger area to reflect more indirect light before entering through the glass pane.

Figure 9 shows that the ASS+ increased the DA up to 4.5%. The greater the collector's angular spread, the greater the improvement of the DA. However, the collector's angular spread only slightly improved the DA. Because of the small contribution of the energy use for lighting and the heat released by electrical lighting to the total building energy consumption, W091_A52_v3 (the lowest CL and Ti) was considered to have the best energy performance.

Real performance of the ASS+

Short-term monitoring of four fenestration models, i.e. UC, CE, ADS and ASS+ on the north-facing aperture of a test building in Yogyakarta (see Figure 11), was carried out to obtain the real comparative daylighting and thermal performance of the ASS+. Monitoring was conducted from September 8 to October 3. During this time, the north-facing clerestories were exposed to the sun. Because of the dense surrounding on the West and East side of the test building, measurements were carried out from 10.30 a.m. – 01.30 p.m. when the sun was located around the zenith. Only data acquired during clear-sky days with similar thermal site conditions were used.

The ratio of the Ei to the outdoor illuminance at the shaded area (Eo) or Ei/Eo from the 4-day measurements (see Figure 12.) shows that ASS+ performed well following the performance of the ADS. It should be noted that the monitoring of the ASS+ recorded lower than Eo the Eo during the monitoring of the ADS.

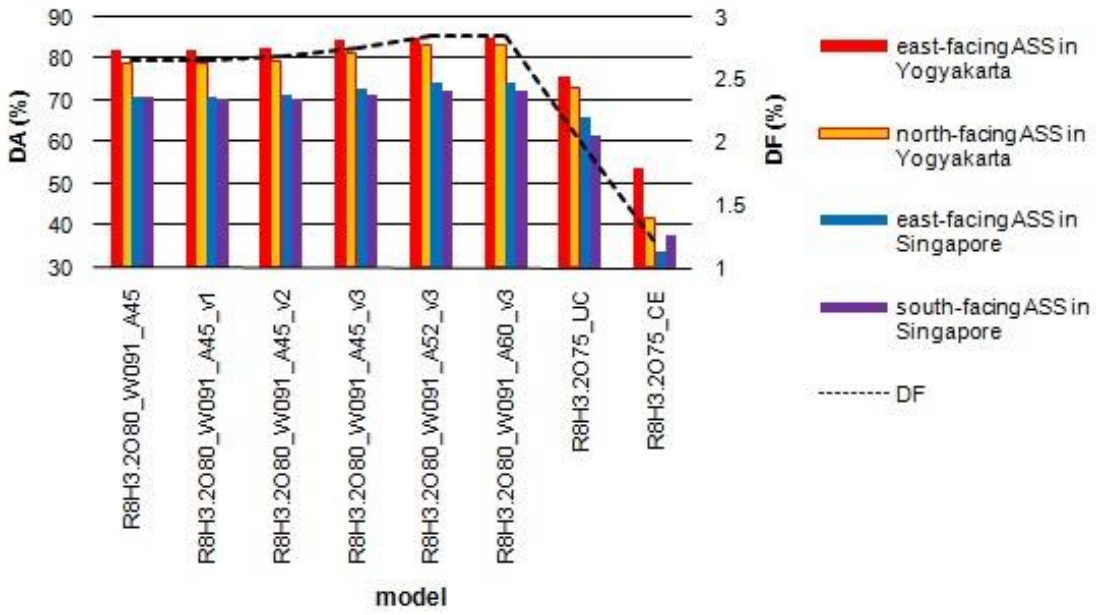

Figure 10: *DF and DA of an indoor space equipped with ASS, UC and CE.*

Figure 11: *The real models (from left to right): UC, CE, ADS, and ASS+.*

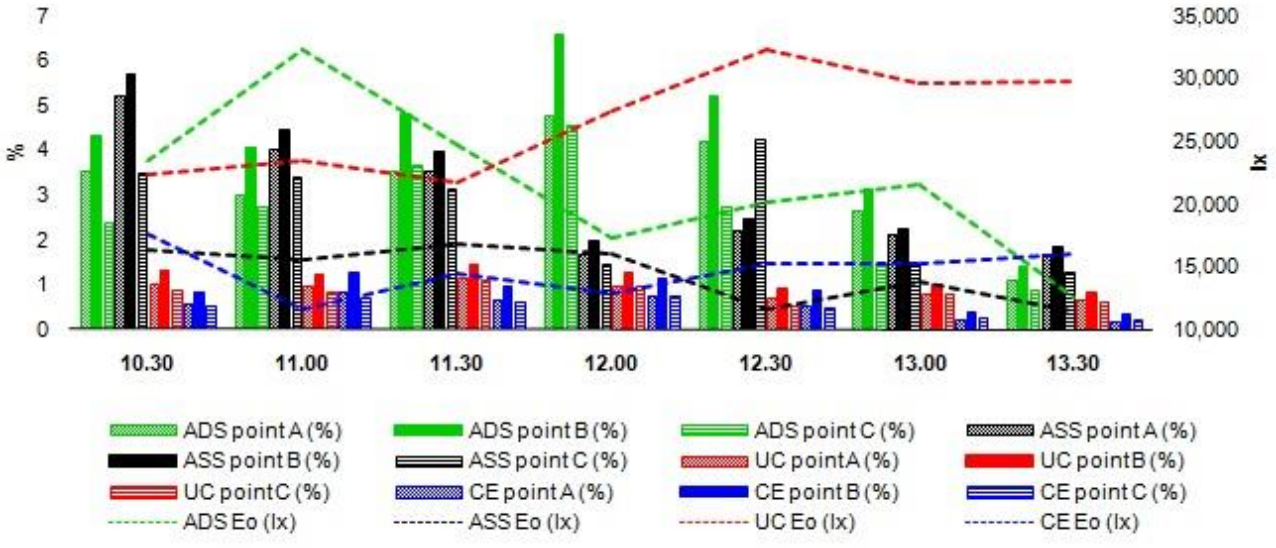

Figure 12: *The measured Ei/Eo of four fenestration models at point A, B and C (in %) and the Eo during measurements (in lx).*

At noon the Ei/Eo of the building equipped with ASS+ decreased substantially. During this time the most of zenithal light beams falling on the collector passed through the cavities rather were reflected by the collector body. The reflected light from the zenith that contributed to the Ei at 12 a.m., hence, reduced significantly in accordance to the percentage of the cavity area. On the contrary, at 10.30-11.00 a.m the cavities let the light beams enter the indoor space, which further created higher Ei/Eo of the ASS+ than the Ei/Eo of the ADS.

Although the monitoring data have been selected based on the similarity in temperature and relative humidity, the global solar radiation data varied from day to day. The wind speed measured during the ADS installation tended to be lower than the wind speed measured during the installation of the other fenestrations. However, there were only slight differences in measured ambient air temperature (To) and relative humidity (Rho) (see Figure 13) with less than 1.4 ^{o}C, 7.2 %, and 0.7 m/s of the deviations of the average To, Rho, and wind velocity deviations for every 30 mins respectively.

Figure 14 shows that the ASS+ produced higher Ti-To at 12.30, 13.00 and 13.30 a.m. than the CE, although the opposite condition occurred at 10.30, 11.00 and 11.30 a.m. due to the cavities on the collector body. In general, a quite good agreement was achieved between the comparative CFD simulation results and the comparative monitoring results. Improvement of the cavities size and position should be discussed in the future study to enhance the performance.

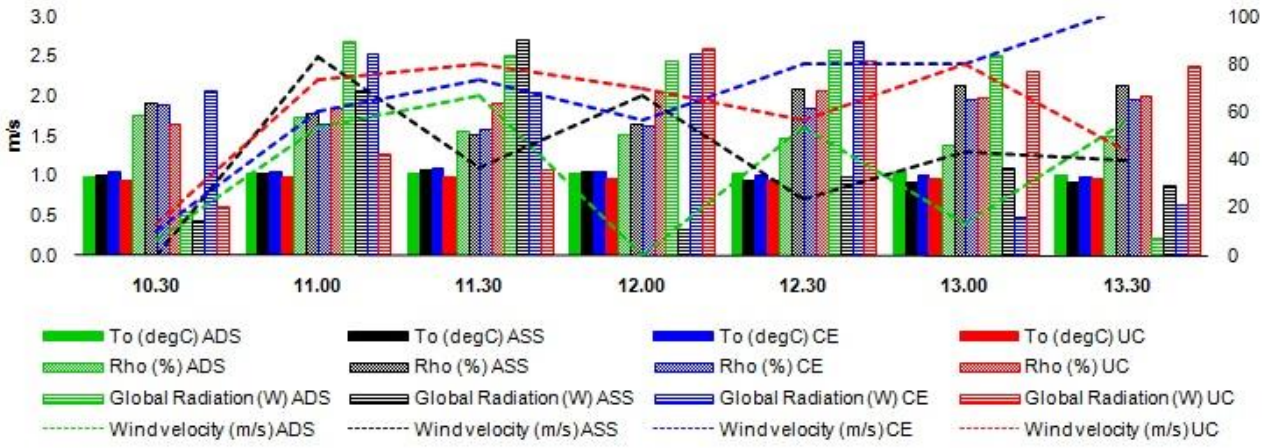

Figure 13: *The outdoor thermal conditions during monitoring*

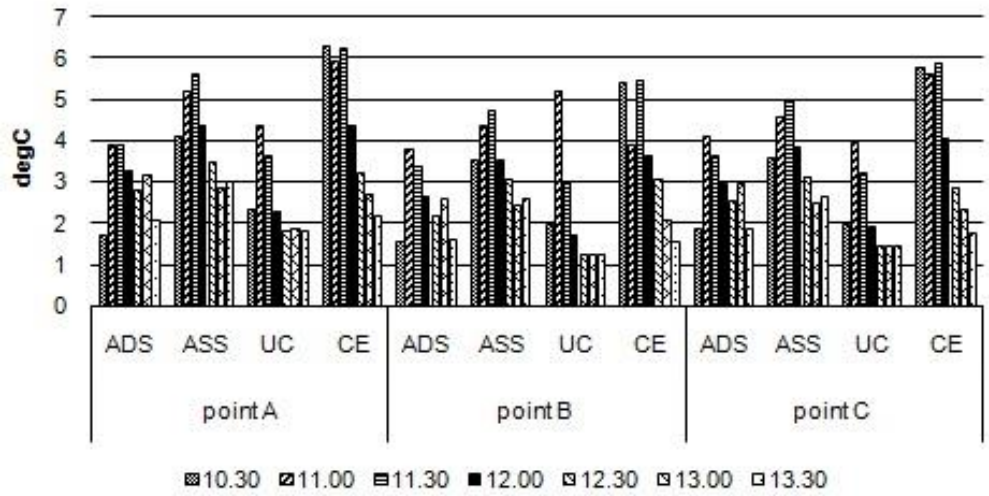

Figure 14: *Temperature difference between indoor and outdoor (Ti-To) of the building equipped with various fenestration models (degC).*

Conclusion

The simulation-based parametric study successfully developed a new solar shading (ASS+) to answer the typical challenge of warm-humid external shading. By adding cavities and self shading on the anidolic collector, the ASS+ could attain high daylighting and thermal performance. A quite good agreement between the comparative simulation results and the comparative short-term monitoring data led to a conclusion that the simulation-based parametric study is quite reliable and the design of ASS+ can be applied to achieve an energy-

efficient and comfortable indoor space in warm-humid climates.

Although DA calculation sufficiently described the annual daylighting performance, yet hourly daylighting and thermal simulations are still required to determine the appropriate position and size of cavities on the collector body for improving the ASS+ energy performance in the next study. To improve the simulation results and more comprehensive study on ASS with varying room sizes, EnergyPlus simulations coupled with more detailed (day)lighting and thermal analysis should be developed for the future study.

Acknowledgement

Authors gratefully acknowledge Universitas Atma Jaya Yogyakarta for the research funding and the Directorate of Higher Education Republic Indonesia, Ministry of Research, Technology and Higher Education in the scheme of *Hibah Bersaing 2015* under the contract number 005/HB-LIT/III/2015 (Government to University) for supporting the monitoring set-up.

References

Binarti, F. and P. Satwiko (2016). Assessing the energy saving potential of anidolic system in the tropics. Submitted to: En Efficiency.

Binarti, F. and P. Satwiko (2016). An east-facing anidolic daylighting system on a tropical urban house. *Indoor and Built Environment* 25(4), 691-702. Doi: 10.1177/1420326X15574787.

Chadwell, R. (1997). The Radiance Lighting Simulation and Rendering System. Lawrence Berkeley Laboratory, Los Angeles, CA. http://radsite.lbl.gov/radiance/refer/long.html (1997, accessed 12 September 2016).

Crawley, D.B., Lawrie, L.K., Winkelmann, F.C., Buhl, W.F., Pedersen, C.O., Strand, R.K., Liesen, R.J., Fisher, D.E., Witte, M.J., Henninger, R.H., Glazer, J., and D. Shirey (2013). EnergyPlus v.8.1, Atlanta, Georgia.

ESI Group (2014). CFD-ACE+ v2014.0: Modules Manual Part I. www.esi-group.com.

Hyde, R. (eds). (2008). Chapter 9: Design, Elements, and Strategies in Bioclimatic Housing: Innovative Designs for Warm Climates. London: Earthscan.

Kleindienst, S.A. (2006). Improving the daylighting conditions of existing buildings: the benefits and limitations of integrating anidolic daylighting systems using the American classroom as a model. Master thesis, Massachusetts Institute of Technology, USA.

Linhart, F., Wittkopf, S.K., and J-L. Scartezzini (2010). Performance of anidolic daylighting systems in tropical climates, parametric studies for identification of main influencing factors. *Solar Energy* 84, 1085–1094.

Loutsenhiser, P.G., Manz, H., Carl, S., Simmler, H., and G.M. Maxwell (2008). Empirical validations of solar gain models for a glazing unit with exterior and interior blind assemblies. *Energy and Buildings* 40, 330-340.

Maestre, I.R., Perez-Lombar, L., Foncubierta, J.L., and P.R. Cubillas (2012). Improving direct solar shading calculations within building energy simulation tools. Building Performance Simulation 1-12.

Mardaljevic, J. (2004). Verification of program accuracy for illuminance modeling: assumptions, methodology and an examination of conflicting findings. *Lighting Res and Tech* 36(3), 217-242.

Marsch, A., 2005. Ecotect Software v.5.5. Square One, Cardiff.

Ng, E. (2001). A study on the accuracy of daylighting simulation of heavily obstructed buildings in Hong Kong. In: *7th International IBPSA Conference*, Rio de Janeiro, Brazil, 13-15 August 2001.

Praditwattanakit, R, Chaiwiwatworakul, P, and S. Chirarattananon (2013). Anidolic concentrator to enhance the daylight use in tropical buildings, Int. Conf. on Alternative Energy in Developing Countries and Emerging Economies. Bangkok, Thailand, 30–31 May 2013. ftp://202.28.64.61/04. (2013, accessed 7 August 2014).

Rahim, R. and R. Mulyadi (2004). Preliminary study of horizontal illuminance in Indonesia. In: *5th SENVAR*, Universiti Teknologi Malaysia, Skudai, Johor, Malaysia, 10–12 December 2004, pp.1-10.

Rea, M.S. (2000). *The IESNA Lighting Handbook: Reference and Application*. New York: Illuminating Engineering Society of North America (IESNA), ch.8, p. 25. Atlanta.

Reinhart, C.F. and P-F. Brexton (2009). *Experimental Validation of Autodesk 3ds Max Design 2009' and Daysim 3.0*. NRC Project # B3241, Milford, USA.

Reinhart, C.F. and O.J. Walkenhorst (2001). Dynamic RADIANCE-based Daylight Simulations for a full-scale Test Office with outer Venetion Blinds. *Energy and Buildings* 38(7), 890-904.

Scartezzini, J-L. and G. Courret (2002). Anidolic daylighting systems. *Solar Energy* 73, 123–135.

University of Illinois and Lawrence Berkeley National Laboratory (2015). EnergyPlus Documentation: Engineering Reference.

Ward, G. (2002). *Desktop Radiance Software*. Lawrence Berkeley Laboratory, California.

Wittkopf, S.K., Grobe, L.O., Compagnon, R., Kampf, J., Linhart, F., and J-L. Scartezzini (2010). Ray tracing study for non-imaging daylight collectors. *Solar Energy* 84, 986–996.